Available online at www.sciencedirect.com
SCIENCE DIRECT®
Journal of Magnetic Resonance 177 (2005) 118–128
JMR Journal of Magnetic Resonance
www.elsevier.com/locate/jmr

Increasing ^{14}N NQR signal by ^{1}H–^{14}N level crossing with small magnetic fields

Kent R. Thurber [a,*], Karen L. Sauer [a,b], Michael L. Buess [c], Christopher A. Klug [a], Joel B. Miller [a]

[a] U.S. Naval Research Laboratory, Washington, DC 20375, USA
[b] Department of Physics and Astronomy, George Mason University, Fairfax, VA 22030, USA
[c] SFA, Lanham, MD 20785, USA

Received 29 June 2005; revised 22 July 2005
Available online 24 August 2005

Abstract

NQR detection of materials, such as TNT, is hindered by the low signal-to-noise ratio at low NQR frequencies. Sweeping small (0–26 mT) magnetic fields to shift the ^{1}H NMR frequency relative to the ^{14}N NQR frequencies can provide a significant increase of the ^{14}N NQR signal-to-noise ratio. Three effects of ^{1}H–^{14}N level crossing are demonstrated in diglycine hydrochloride and TNT. These effects are (1) transferring ^{1}H polarization to one or more of the ^{14}N transitions, including the use of an adiabatic flip of the ^{1}H polarization during the field sweep, (2) shortening the effective ^{14}N T_1 by the interaction of ^{1}H with the ^{14}N transitions, (3) "level transfer" effect where the third ^{14}N (spin 1) energy level or other ^{14}N sites with different NQR frequency are used as a reservoir of polarization which is transferred to the measured ^{14}N transition by the ^{1}H. The ^{14}N NQR signal-to-noise ratio can be increased by a factor of 2.5 for one ^{14}N site in diglycine hydrochloride (and 2.2 in TNT), even though the maximum ^{1}H frequency used in this work, 1116 kHz, is only 30% larger than the measured ^{14}N frequencies (834 kHz for diglycine hydrochloride and 843 kHz for TNT).
Published by Elsevier Inc.

Keywords: NMR; NQR; Double resonance; Level crossing; ^{14}N; TNT; Diglycine hydrochloride

1. Introduction

NQR detection of hidden materials, such as TNT (trinitrotoluene), has several favorable features. NQR is a bulk technique and can detect fully enclosed material, as long as the container does not completely block the RF magnetic field. Since the quadrupolar frequencies are specific to the crystal structure, false alarms are limited [1]. However, ^{14}N NQR detection of TNT is hindered by the low signal-to-noise ratio at low NQR frequencies. To increase the signal-to-noise ratio, double resonance techniques have been applied to TNT [2–5]. Double resonance techniques can increase the signal, at the cost of requiring a magnetic field. Most of these techniques have used the ^{1}H nuclei as an indirect detector of the ^{14}N resonance. An alternative approach is to measure the ^{14}N NQR directly while using the ^{1}H nuclei to increase the ^{14}N signal. One way to do this is to polarize the ^{1}H at high field and transfer the polarization to the ^{14}N by energy level crossings as the magnetic field is reduced. This basic level-crossing technique has been successfully tested on a few nitrogen-containing compounds [5–7].

In these experiments, we use small magnetic fields to explore the basic level-crossing technique and other related methods that use the neighboring ^{1}H to

* Corresponding author. Fax: +1 301 496 0825.
E-mail addresses: thurberk@niddk.nih.gov, kentt@alum.mit.edu (K.R. Thurber).

1090-7807/$ - see front matter. Published by Elsevier Inc.
doi:10.1016/j.jmr.2005.07.016

increase the measured ^{14}N NQR signal. The small (0–26 mT) magnetic fields are easily provided by a simple home-built solenoid. We demonstrate the significant increase of the ^{14}N NQR signal in a test compound, diglycine hydrochloride [8], and in TNT. The demonstrated effects are (1) transferring ^{1}H polarization to one or more of the ^{14}N transitions, including an adiabatic flip of the ^{1}H polarization during the field sweep when beneficial, (2) shortening the effective ^{14}N T_1 by the interaction of ^{1}H with the ^{14}N transitions, (3) "level transfer" effect where the unmeasured third ^{14}N (spin 1) energy level or other ^{14}N sites with different NQR frequency are used as a reservoir of polarization which is transferred to the measured ^{14}N transition by the ^{1}H. The best ^{14}N NQR signal-to-noise ratio was achieved in both diglycine hydrochloride and TNT by using both effects 2 and 1: first, matching the ^{1}H Zeeman frequency to the measured ^{14}N NQR frequency to shorten ^{14}N T_1, and then, transferring ^{1}H polarization to ^{14}N at the other two level crossings. The signal-to-noise ratio for a fixed amount of time can be increased by a factor of 2.5 for the ^{14}N site 2 of diglycine hydrochloride, and increased by 2.2 for the ^{14}N signal near 843 kHz of TNT, even though the maximum ^{1}H frequency used in this work, 1116 kHz, is only 30% larger than the measured ^{14}N frequencies (834 kHz for diglycine hydrochloride and 843 kHz for TNT).

2. Background

The quadrupolar Hamiltonian is [9]

$$\mathscr{H} = \frac{e^2qQ}{4I(2I-1)}\left\{3I_Z^2 - I(I+1) + \frac{1}{2}\eta(I_+^2 + I_-^2)\right\}, \qquad (1)$$

where $eq = V_{ZZ}$, the largest component of the electric field gradient tensor in the principal axes frame, $\eta = (V_{XX} - V_{YY})/V_{ZZ}$, eQ is the quadrupole moment of the nucleus and I is the spin of the nucleus. As a spin 1 nucleus with $\eta \neq 0$ (η ranges from 0.17 to 0.30 in these samples), the ^{14}N nucleus has three energy levels, given below with their associated eigenstates. The eigenstates are written in terms of the spin states of I_Z, where the Z axis is defined above by the quadrupolar principal axes frame.

$$\begin{aligned} E_{|Y\rangle} &= h\nu_Q\left(\frac{1+\eta}{3}\right); \quad |Y\rangle = \frac{1}{\sqrt{2}}(|+1\rangle + |-1\rangle), \\ E_{|X\rangle} &= h\nu_Q\left(\frac{1-\eta}{3}\right); \quad |X\rangle = \frac{1}{\sqrt{2}}(|+1\rangle - |-1\rangle), \\ E_{|Z\rangle} &= h\nu_Q\left(\frac{-2}{3}\right); \quad |Z\rangle = |0\rangle, \end{aligned} \qquad (2)$$

where

$$\nu_Q = \frac{3e^2qQ}{4h}. \qquad (3)$$

In our qualitative discussions of the level-crossing effects, we will often assume that $e^2qQ > 0$ and thus $\nu_Q > 0$. However, the sign of ν_Q does not change the results of the level-crossing effects given the approximations used in our later analysis in this article. From the three ^{14}N energy levels, the three resulting frequencies are

$$\nu_+ = |Y\rangle \rightarrow |Z\rangle = \nu_Q\left(1 + \frac{\eta}{3}\right), \qquad (4)$$

$$\nu_- = |X\rangle \rightarrow |Z\rangle = \nu_Q\left(1 - \frac{\eta}{3}\right), \qquad (5)$$

$$\nu_0 = |Y\rangle \rightarrow |X\rangle = \nu_Q\left(\frac{2\eta}{3}\right). \qquad (6)$$

The first basic effect that we can use to increase the ^{14}N NQR signal-to-noise ratio is the transfer of polarization from the ^{1}H to the ^{14}N at the magnetic fields where the ^{1}H Zeeman frequency is equal to one of the three ^{14}N NQR frequencies [10]. A small DC magnetic field primarily changes the ^{1}H frequency, while the ^{14}N NQR frequencies are just slightly shifted, broadening the NQR transitions in a powder sample [3,11]. This is for two reasons: first, because the gyromagnetic ratio is much larger for ^{1}H (42.6 MHz/T) than for ^{14}N (3.08 MHz/T); and second, the ^{14}N NQR energy levels do not shift to first order in the field [12] because the expectation value of the magnetic moment is zero in all directions. (The zero expectation value of the magnetic moment in the Z direction can be seen in the eigenstates given in Eqs. (2).) Because there are three ^{14}N NQR frequencies, there are three magnetic fields where avoided energy level crossing occurs, as can be seen in Fig. 1. At these level crossings, the ^{1}H Zeeman

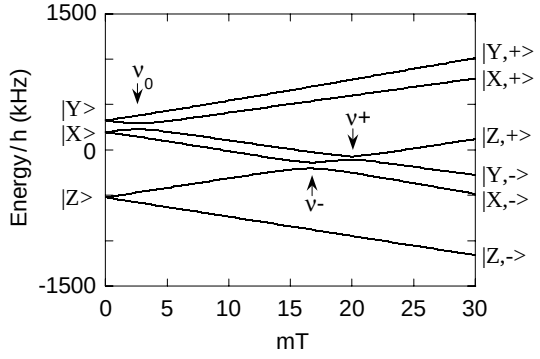

Fig. 1. Energy levels as a function of magnetic field for one ^{14}N and one ^{1}H that are dipole-coupled. The energy states are labeled at the right (high field) side with the ^{14}N state (X, Y, or Z) and the ^{1}H state (+ or −). The arrows indicate the three avoided energy level crossings, where the ^{1}H frequency equals one of the three ^{14}N frequencies (ν_+, ν_-, or ν_0). This specific example of the energy levels has the magnetic field along the ^{14}N quadrupolar Z axis; and the internuclear vector is in the quadrupolar XZ plane and makes an angle of $\pi/3$ with the Z axis. The dipole coupling, $\gamma_H\gamma_N h/4\pi^2 r_{NH}^3$, is shown as 50 kHz, larger than estimated in these materials (7.3 kHz for glycine [13]), in order to show the avoided level crossings clearly. The ^{14}N quadrupole coupling is that of site 2 of diglycine hydrochloride ($\nu_Q = 780$ kHz, $\eta = 0.21$).

frequency equals one of the three ^{14}N NQR frequencies. If there was no ^{1}H–^{14}N dipole interaction, the energy levels would cross; with a dipole coupling, the energy levels avoid crossing each other with a minimum splitting determined by the strength of the dipole coupling. For our measurements of diglycine hydrochloride and TNT, these level crossings are roughly at 20 mT for ν_+, 17 mT for ν_-, and 2.5 mT for ν_0. At a level crossing, efficient transfer of polarization between the ^{1}H transition and the corresponding ^{14}N transition can occur via the ^{1}H–^{14}N dipole interaction because the energies of the two transitions are equal. Generally, the sequence of these experiments is as follows (see Fig. 2). First, a small DC magnetic field is applied which polarizes the ^{1}H. Then, the magnetic field is swept down through the level crossings, transferring polarization to the ^{14}N nuclei. If necessary, the field sweep can be paused at the level crossings to allow more time for polarization transfer. Finally, the ^{14}N NQR signal is measured at zero field with a spin-lock, spin-echo (SLSE) sequence [14].

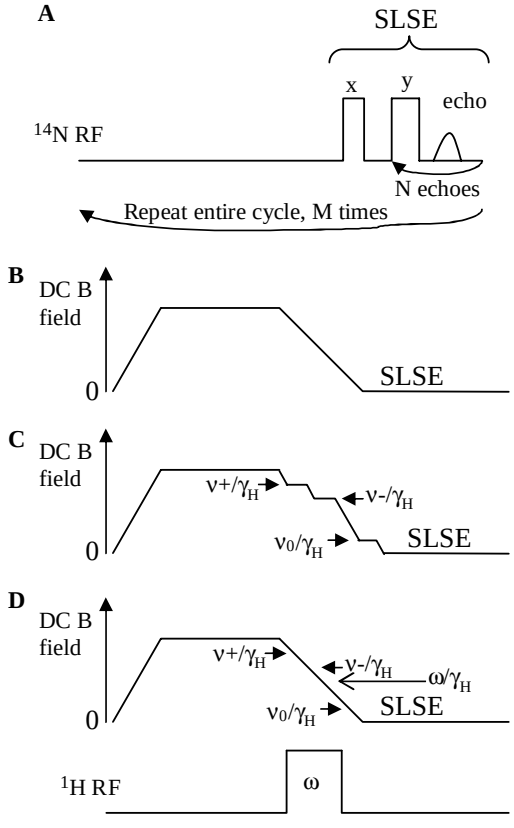

Fig. 2. NQR sequences: (A) spin-lock spin-echo (SLSE) pulse sequence used for ^{14}N NQR at zero field, (B) continuous field sweep across ^{1}H–^{14}N level crossings, (C) field sweep with stops at the level crossings, and (D) field sweep with RF magnetic field applied during the sweep to cause an adiabatic flip of ^{1}H polarization between level crossings.

3. Experimental

Two samples were used in these experiments: diglycine hydrochloride and trinitrotoluene (TNT). Diglycine hydrochloride, $2(C_2H_5O_2N)\cdot HCl$, was used as a test compound because it has ^{14}N NQR frequencies close to those of TNT, a fast T_1 for rapid data collection, and ^{1}H bonded to the ^{14}N (the NH_3 group) to provide significant ^{1}H–^{14}N dipole coupling. There are 11/2 total ^{1}H per ^{14}N. We should note that despite the term "diglycine" in the compound name, which often refers to compounds where the two glycine amino acids are chemically linked, diglycine hydrochloride has simply two unlinked molecules of glycine for every molecule of HCl. However, the two nitrogen sites in the two glycine molecules do have slightly different NQR frequencies. Each ^{14}N crystal site has three ^{14}N NQR frequencies, ν_+, ν_-, and ν_0. The ^{14}N NQR frequencies of both diglycine hydrochloride and the orthorhombic phase of TNT were matched as ν_+, ν_-, ν_0 triples (see Table 1) by measuring T_{2e}, the decay of the spin-lock spin-echo train. When the ^{1}H Zeeman frequency matches the ν_0 ^{14}N NQR frequency, T_{2e} decreases for the associated ν_+ and ν_- transitions [16]. All of the diglycine hydrochloride data in this article are from site 2 ($\nu_+ = 834$ kHz, $\nu_- = 725$ kHz, $\nu_0 = 109$ kHz). The experiments used approximately 23 g diglycine hydrochloride from Sigma and were typically run for 3000 cycles (M, Fig. 2) or more, taking $\geqslant$15 min.

Trinitrotoluene, 2,4,6-$(NO_2)_3C_6H_2(CH_3)$, has two crystalline forms, orthorhombic and monoclinic. Each crystal type has 6 nitrogen sites with different NQR frequencies (see Table 1) [16]. There are 5/3 total ^{1}H per ^{14}N. Fig. 3 has low-resolution spectra of the ν_+ and ν_- frequencies of the TNT sample. The sample is roughly 40 mL ($\sim$25 g) of TNT flakes immersed in water for safety. It is primarily orthorhombic, but does contain some monoclinic component. The spectra shown (Fig. 3) were acquired in 6000 cycles (M, Fig. 2) or more ($\geqslant$8 h). However, signal sufficient for reasonable spectra could be acquired in 1000 cycles.

The solenoid to provide the DC magnetic field is a hand-wound coil with a notch design [17]: two complete winding layers, with added extra turns at each end to increase homogeneity. The resulting coil (7 cm diameter, 11.5 cm length) provides 2.15 mT/A, with homogeneity of 0.2% for the diglycine hydrochloride sample shape and 1.5% for the longer TNT sample. The coil resistance is 1.2 Ω and the inductance is 3 mH. The magnetic field control for the level-crossing sequences uses a 12 bit digital number from a Tecmag Aries spectrometer. This digital value is converted to an analog voltage, and that voltage determines the current output of a Kepco power supply. The maximum field is limited to 26 mT by the 12 A maximum output of the power supply, while the sweep rate is limited to $\sim$2.5 mT/ms by the coil

Table 1
^{14}N NQR frequencies (in kHz) for orthorhombic and monoclinic TNT and diglycine hydrochloride

	ν_+ (kHz)	ν_- (kHz)	ν_0 (kHz)	
Orthorhombic	838.8	742.7	96.1	
TNT	843.6	754.0	89.6	
	847.4	713.3	134.1	
	849.5	742.7	106.8	
	863.4	770.5	92.9	
	869.4	717.4	152.0	
Monoclinic	838.3	740.7 or 744.3	97.6 or 94.0	
TNT	844.4	753.6	90.8	
	845.3	715.2	130.1	
	849.9	740.7 or 744.3	109.2 or 105.6	
	861.3	770.3	91.0	
	871.3	715.2	156.1	
Diglycine	982	815	167	Site 1
hydrochloride	834	725	109	Site 2

TNT frequencies are at 13 °C, interpolated or extrapolated from [15]. Diglycine hydrochloride frequencies from this work are at room temperature.

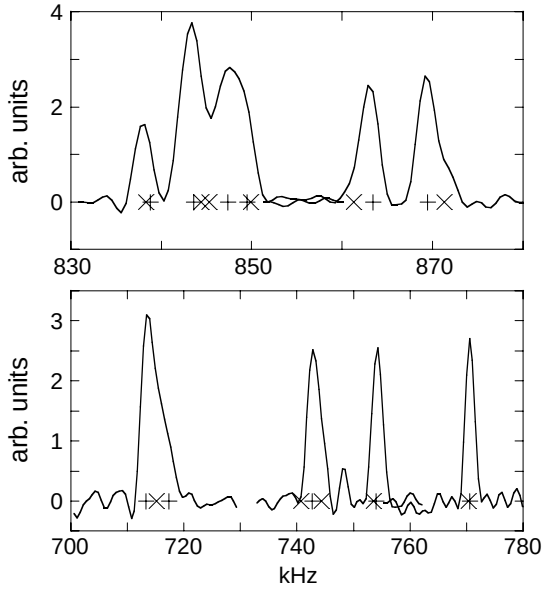

Fig. 3. ^{14}N NQR low-resolution spectra from TNT in water, ν_+ lines (838–871 kHz) and ν_- lines (713–770 kHz). Also shown are the expected line positions for orthorhombic (+) and monoclinic (×) TNT, extracted from [15] (see Table 1). The relative intensities of different lines are strongly affected by the bandwidth of the spin-lock spin-echo (SLSE) sequence. Spectra taken at 13–16 °C.

inductance and the sweep response of the power supply. The magnet is water cooled with coiled copper tubing. For the TNT experiments, the sample region was also water cooled with copper tubing. The TNT sample had a temperature gradient of $\leqslant$2 °C across the sample when the magnet was warm. Experimental sequences with and without magnetic field were always interleaved, so that the signal change is compared between sequences done in the same experiment. This avoids any effect of both temperature and electronic changes over time. For the diglycine hydrochloride data in this article, the RF field B_1 was perpendicular to the DC field B_0. Selected sequences were also run with B_1 parallel to B_0, and there were no significant differences ($\leqslant$8%). The TNT measurements were done with B_1 parallel to B_0.

4. Results

4.1. Level-crossing effect

Fig. 4 shows the diglycine hydrochloride ^{14}N NQR signal measured after a magnetic field sweep, normalized by the signal measured without any magnetic field sweep. The DC magnetic field was applied for 500 ms (>4 ^{14}N T_1) in order to include just the level-crossing effect and not the T_1 effects discussed later. The results are plotted as a function of the applied magnetic field (in units of the ^{1}H frequency). With the highest field sweep used (26 mT), the signal for ν_+ is 60% larger than without any field sweep. For TNT, we found that simply sweeping the magnetic field at about 100 kHz/ms (2.5 mT/ms) through the level crossings gave a minor signal increase (20%). However, if the field sweep is paused at each of the level crossings (Fig. 2C), the signal increase is larger. The need to spend more time at the level crossing to achieve polarization transfer has been seen in other ^{14}N double resonance experiments on samples with NO_2 groups [18]. This is presumably a result of weak ^{1}H–^{14}N dipole couplings in TNT. We estimate

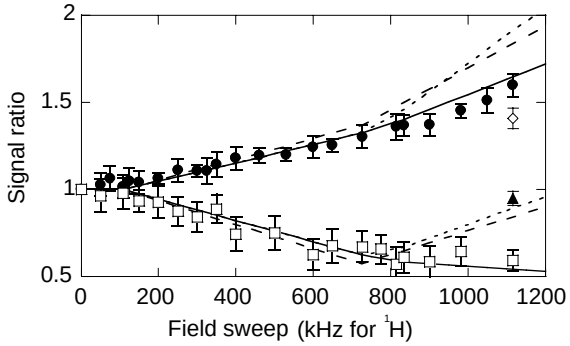

Fig. 4. ^{14}N NQR signal after magnetic field applied for 500 ms ($\gg^{14}$N T_1) (normalized by signal without any field sweep) as a function of the magnetic field strength (in units of the ^{1}H frequency). Data shown for diglycine hydrochloride site 2 ^{14}N, ν_+ (●) (834 kHz), and ν_- (□) (725 kHz) (sequence Fig. 2B). The signal increase when a RF field is applied at 607 kHz to produce an adiabatic passage of the ^{1}H nuclei during the field sweep is shown for ν_+ (▲) and ν_- (◇) (sequence Fig. 2D). Lines show calculations of signal increase from transfer of ^{1}H polarization: dashed line, adiabatic avoided level crossings with one ^{1}H and one ^{14}N; dotted line, spin temperature equilibration at level crossings with 5 ^{1}H per ^{14}N; solid line, spin temperature model with higher two crossings (at 834 and 725 kHz) only 25% effective. The total cycle time was 525 ms. Data were taken at 33 °C (ν_+), 37–43 °C (ν_-), and 31 °C (adiabatic passage).

that the ^{1}H–^{14}N dipole couplings in TNT are $\lesssim$500 Hz, more than 10 times smaller than estimated for pure glycine (7.3 kHz) [13]. We found that spending 100 ms or more at the level crossing provided good polarization transfer for TNT. For a sweep from 26 mT (1116 kHz) with 100 ms stops at all the level crossings for the four orthorhombic lines around 843 kHz, the total TNT signal around 843 kHz at 15 °C was a factor of 2.1 times larger than without any field sweep. The 12 stops for the three level crossings of each of the four lines around 843 kHz were reduced to seven stops by stopping only once for closely spaced lines. The stops were at 854 kHz for the 4 ν_+ crossings (shifted from 843 kHz to account for magnetic field broadening), 754, 743 (2 lines), and 715 kHz for the ν_- crossings, and 132, 107, and 93 kHz (2 lines) for the ν_0 crossings.

This basic level-crossing effect has been reviewed several times [6,10,11,19–21], though often from the point of view of measuring the ^{1}H NMR, rather than the ^{14}N NQR. One model for the level-crossing effect is from a spin temperature approach [10]. In this model, at each level crossing, when the ^{1}H Zeeman frequency is equal to one of the ^{14}N NQR frequencies, those two transitions come into thermal equilibrium with each other. We derive the spin temperature model as follows. Let N_H and N_N be the number of interacting ^{1}H and ^{14}N nuclei. The initial populations of the two ^{1}H levels are approximated as $\frac{N_H}{2}(1-x)$ and $\frac{N_H}{2}(1+x)$ in the high temperature limit with $x=\frac{h\nu_H}{2kT}$. ν_H is the frequency where the ^{1}H were in thermal equilibrium with temperature T. The initial populations of the ^{14}N levels are $\frac{N_N}{3}(1+a)$, $\frac{N_N}{3}(1+b)$, and $\frac{N_N}{3}(1+c)$, for the $|Y\rangle$, $|X\rangle$, and $|Z\rangle$ states, respectively, with

$$a=-\frac{E_{|Y\rangle}}{kT}=-\frac{h\nu_Q(1+\eta)}{3kT}, \tag{7}$$

$$b=-\frac{E_{|X\rangle}}{kT}=-\frac{h\nu_Q(1-\eta)}{3kT}, \tag{8}$$

$$c=-\frac{E_{|Z\rangle}}{kT}=\frac{2h\nu_Q}{3kT}. \tag{9}$$

Using conservation of the number of ^{1}H and ^{14}N nuclei, conservation of the energy, and the high temperature limit, this model leads to equations for the new population differences after the level crossing, x_{new}, a_{new}, b_{new}, and c_{new}. For example, the following equations are for a level crossing with the ν_+ ^{14}N frequency [10,19]

$$p=\frac{N_H}{N_H+\frac{2}{3}N_N}, \tag{10}$$

$$x_{new}=(1-e(1-p))x+e(1-p)\left(\frac{c-a}{2}\right), \tag{11}$$

$$a_{new}=-epx+\left(1-\frac{1}{2}ep\right)a+\frac{1}{2}epc, \tag{12}$$

$$b_{new}=b, \tag{13}$$

$$c_{new}=epx+\frac{1}{2}epa+\left(1-\frac{1}{2}ep\right)c. \tag{14}$$

The parameter, e, describes whether the transition comes into complete thermal equilibrium. If $e=1$, the ^{1}H and the ^{14}N transition have fully equilibrated; if $e=0$, nothing happens at the level crossing. The factor of 2/3 in p arises from the fact that the ^{1}H are coming into equilibrium with one of the ^{14}N transitions, which involves two out of the three ^{14}N energy levels, thus only $\approx$2/3 of the ^{14}N nuclei are involved in the high temperature limit. In this model of a level crossing, two of the ^{14}N energy levels thermally equilibrate with the two ^{1}H energy levels, while the population of the third ^{14}N energy level does not change. The other two level crossings at ν_- and ν_0 result in similar equations when derived with the assumptions of the spin temperature model. The results for several consecutive level crossings can be modeled by using the new values of x, a, b, and c as the initial conditions for the next level crossing. An example of the calculations with the spin temperature model is shown in Fig. 5. To first order in N_N/N_H and the population differences, and assuming complete thermal equilibrium for all three level crossings, the ^{14}N NQR signal after a field sweep, normalized by the signal without any field sweep, S_{new}/S, is given in [6],

$$(S_{new}/S)_{\nu_+}=\frac{1}{8}\left[13\frac{\nu_H}{\nu_+}-2\frac{\nu_-}{\nu_+}+1+\left(9+8\frac{\nu_-}{\nu_+}-21\frac{\nu_H}{\nu_+}\right)\frac{N_N}{N_H}\right], \tag{15}$$

$$(S_{new}/S)_{\nu_-}=\frac{1}{8}\left[5\frac{\nu_H}{\nu_-}+\frac{\nu_+}{\nu_-}-2+\left(4+3\frac{\nu_+}{\nu_-}-3\frac{\nu_H}{\nu_-}\right)\frac{N_N}{N_H}\right], \tag{16}$$

$$(S_{new}/S)_{\nu_0}=\frac{1}{8}\left[8\frac{\nu_H}{\nu_0}+\left(6\frac{\nu_+}{\nu_0}+4\frac{\nu_-}{\nu_0}-18\frac{\nu_H}{\nu_0}\right)\frac{N_N}{N_H}\right]. \tag{17}$$

Without going through the detailed calculations, the general nature of the change in signal for the ^{14}N transitions can be seen qualitatively (see Fig. 5). As the field is reduced from high field with polarized ^{1}H, the first level crossing is with the highest ^{14}N NQR frequency ($\nu_+=|Y\rangle\rightarrow|Z\rangle$). At this level crossing, the population of $|Z\rangle$ is increased and $|Y\rangle$ decreased. At each level crossing, the ^{1}H polarization is reduced by the amount of energy transfer to the ^{14}N. However, the ^{1}H polarization is reduced by very little if there are many ^{1}H per ^{14}N. At the second level crossing with the middle ^{14}N NQR frequency ($\nu_-=|X\rangle\rightarrow|Z\rangle$), the population of $|Z\rangle$ is again increased and $|X\rangle$ decreased. At the third level crossing with the lowest ^{14}N NQR frequency ($\nu_0=|Y\rangle\rightarrow|X\rangle$), the population of $|X\rangle$ is now increased, and $|Y\rangle$ decreased. For the $\nu_+=|Y\rangle\rightarrow|Z\rangle$ transition, the

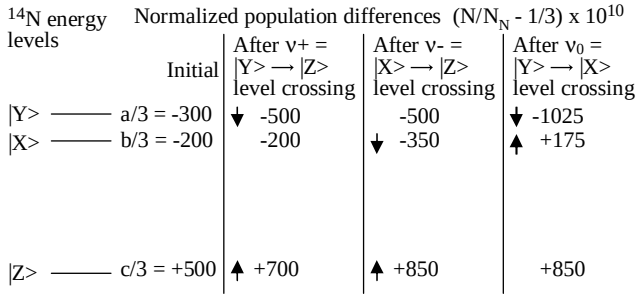

Fig. 5. Example of the ^{14}N energy level population differences during a level-crossing field sweep using the spin temperature model. The population differences given are the differences from the uniform 1/3 of the nuclei in each energy level. The differences are normalized by the total number of ^{14}N nuclei (N_N) and are multiplied by 10^{10}. For numerical simplicity, this example is for $\nu_Q = 750$ kHz, $\eta = 0.20$, $T = 160$ K, the ^{1}H polarized at $\nu_H = 1200$ kHz, many protons per nitrogen ($N_N/N_H \to 0$), and complete thermal equilibration between ^{1}H and ^{14}N at the level crossings. At each level crossing, the nitrogen transition involved polarizes to a normalized population difference of 1200×10^{-10}. The resulting theoretical signal increase is $(850 + 1025)/(500 + 300) = 2.34$ for ν_+, $(850-175)/(500 + 200) = 0.96$ for ν_-, and $(175 + 1025)/(-200 + 300) = 12$ for ν_0.

population of $|Z\rangle$ has been increased twice and $|Y\rangle$ decreased twice, so the signal is increased as seen in Fig. 4. For the $\nu_- = |X\rangle \to |Z\rangle$ transition, the population of $|Z\rangle$ has been increased twice, but the $|X\rangle$ population has been shifted in both directions, so qualitatively, the signal change could be either positive or negative, and is negative in the low field used in our experiments as seen in Fig. 4. For the $\nu_0 = |Y\rangle \to |X\rangle$ transition, the population of $|Y\rangle$ has been decreased twice, but the $|X\rangle$ population has been shifted in both directions, so qualitatively, the signal change could be either positive or negative. However, the last level crossing is with the ν_0 transition, so after the level crossings, the ν_0 transition is in equilibrium with the proton polarization. This can be seen in the first term of Eq. (17), where $(S_{new}/S)_{\nu_0} = \nu_H/\nu_0$ for many ^{1}H per ^{14}N (N_N/N_H small). So generally, the ν_0 signal will be strongly increased, for example by a factor of 12 for the case calculated in Fig. 5.

The ν_- signal decreases for a complete set of level crossings with our small magnetic fields. However, if one desires an increase in the ν_- signal, this can be done by an adiabatic flip of the ^{1}H polarization during the field sweep (see sequence D in Fig. 2). A RF magnetic field is applied at a frequency in between the ν_- and ν_0 frequencies. The ν_+ and ν_- level crossings are done normally with positive ^{1}H polarization, which benefits the NQR ν_- signal. Then, as the field sweeps down, the ^{1}H nuclei pass through resonance with the RF field. The result is an adiabatic rapid passage done by sweeping the magnetic field, rather than sweeping the RF frequency. The ^{1}H polarization is flipped to negative by the passage. The ν_0 level crossing is then beneficial to the ν_- signal (and detrimental to the ν_+ signal). The result of such a field sweep with RF is shown by the second set of symbols (▲, ◇) at 1116 kHz in Fig. 4. The ν_- signal (◇) is increased, and the ν_+ signal (▲) is not increased. Thus, for diglycine hydrochloride, either ν_+ or ν_- signal can be increased with a DC field sweep: ν_+ without a RF field, and ν_- with a RF field. For TNT, the ν_- signal can be increased simply by choosing to stop and allow time for polarization transfer only at the level crossings that are beneficial to the ν_- signal. This implies not stopping at the ν_0 level crossing. For example, the TNT ν_- signal at 743 kHz was increased by 80% by a field sweep from 1116 kHz field that just stopped at ν_- (743 kHz) (100 ms stop, 5 s cycle time at 15 °C).

The simple spin temperature model fits the diglycine hydrochloride data (Fig. 4) well for the lower field sweeps which only cross the lowest frequency (ν_0) level crossing. For field sweeps which cross the two higher field level crossings, an acceptable fit to the data results if the two higher level crossings are assumed to proceed only 25% of the way to equilibrium. Another way to show that the two higher level crossings are not providing very much signal enhancement under these conditions is to measure the enhancement without crossing the lowest level crossing (ν_0). As mentioned earlier, a full field sweep from 1116 kHz to 0 increases the ν_+ signal by 60% relative to measurement at 0 field without a field sweep. We can also sweep the field from 1116 kHz and stop at 300 kHz (above the ν_0 level crossing at 109 kHz). Then, measuring the ^{14}N NQR at a field of 300 kHz (7 mT) shows an increase of the ν_+ signal by only 13% relative to measurement at 7 mT field without a field sweep. These results demonstrate 13% signal benefit from the two higher level crossings, and approximately 60%–13% = 47% from the lowest crossing. The spin temperature model for 5 ^{1}H per ^{14}N would suggest 42% signal benefit from the two higher level crossings, and 91%–42% = 49% from the lowest crossing. This again clearly suggests that the lowest level crossing is providing signal enhancement as expected from the spin temperature model, but that the higher two level crossings are not. The most likely reason for the low polarization transfer at the higher two level crossings seems to be that the field sweep is too fast to allow full thermal equilibrium between the ^{1}H and ^{14}N transitions. However, because of the fast ^{1}H T_1 (7–10 ms) of diglycine hydrochloride, stopping or slowing the field sweep to allow for full thermal equilibrium between the ^{1}H and ^{14}N, also results in more ^{1}H relaxation during the sweep. We should note that even for complete thermal equilibrium, the most important level crossing is the lowest crossing (ν_0), for our very small magnetic fields.

The simple spin temperature model ignores any effects from energy in the dipole couplings [22], and any effects caused by a finite number of coupled spins. Another useful model for the level crossing with different assumptions is an energy level avoided crossing

model. Fig. 1 shows the energy levels of one ^{14}N and one ^{1}H as a function of magnetic field. The energy level crossings become avoided crossings because of the dipole coupling between the ^{14}N and the ^{1}H. First, the magnetic field is set above the level crossings, and the populations of the energy levels allowed to come into thermal equilibrium. Then as the field is reduced, the populations will follow the energy levels if relaxation effects can be neglected and the field sweep is slow enough to be adiabatic. To be specific, the populations of the $|Y,+\rangle$ and $|X,+\rangle$ states will end up in the $|Y\rangle$ ^{14}N state, $|Z,+\rangle$ and $|Y,-\rangle$ populations will end up in the $|X\rangle$ state, and $|X,-\rangle$ and $|Z,-\rangle$ populations will end up in the $|Z\rangle$ state. As a result, the ^{14}N polarization is increased at zero field. On the other hand, a field sweep fast enough to be completely diabatic will not polarize the ^{14}N at all. For a completely diabatic sweep, the populations of the $|Y,+\rangle$ and $|Y,-\rangle$ states will end up in the $|Y\rangle$ ^{14}N state, and similarly for $|X\rangle$ and $|Z\rangle$. In this case, the ^{14}N polarization does not benefit from the ^{1}H polarization.

The adiabatic condition can be expressed generally as [22]

$$A = \frac{(\Delta\omega_{\min})^2}{\frac{d\omega}{dt}} \gg 1, \tag{18}$$

where $\Delta\omega_{\min}$ is the smallest frequency difference between the states and $d\omega/dt$ is the rate of change of the frequency. Of course, the probability of an adiabatic transition can be more precisely specified [23], but that is beyond the scope of this article. In our case, $\Delta\omega_{\min}$ is roughly 2π times the dipole frequency, ν_{NH}. The splitting, $\Delta\omega_{\min}$, will depend on the angle between the magnetic field and the dipole coupling axis, and so will vary for different crystallites in the powder. Another way of looking at this adiabatic condition is that the time spent in the level crossing region, $2\pi\nu_{NH}/(d\omega/dt)$, must be long relative to the characteristic time for the dipole interaction to operate, $1/\nu_{NH}$ [24].

$$\frac{2\pi\nu_{NH}}{\frac{d\omega}{dt}} \gg \frac{1}{2\pi\nu_{NH}}. \tag{19}$$

For pure glycine, the ^{1}H–^{14}N dipole coupling was estimated as 7.3 kHz [13]. The sweeping magnetic field produces a change in the ^{1}H frequency of approximately 100 kHz/ms, so the adiabatic parameter is $\approx(2\pi \cdot 7.3\times10^{3})^2/(2\pi \cdot 100\times10^{6}) = 3$ for diglycine hydrochloride. For TNT, the dipole couplings are estimated to be $\lesssim$500 Hz, more than 10 times smaller than in diglycine hydrochloride. This results in an estimated adiabatic parameter of $A \lesssim 0.02$, so A is clearly not $\gg$1 for TNT. Thus, in this adiabatic model, the diglycine hydrochloride experiments are expected to be borderline adiabatic, while for TNT the level crossings during the swept field will not be adiabatic. This is consistent with the observation that stopping at the level crossings is required for significant polarization transfer to occur in TNT.

The connection between the avoided level crossing and spin temperature models can be made. The spin temperature model with complete thermal equilibration approaches, in the limit of many coupled spins and high temperature, the result for equalizing the populations of the pairs of energy levels that almost cross at each avoided level crossing. The spin temperature model can result naturally if the relaxation is fast enough to equalize the populations between the energy levels when split by the ^{1}H–^{14}N dipolar coupling only, but the relaxation is negligible when the energy splitting is larger. The relaxation of the ^{1}H–^{14}N dipolar order may happen by interactions between the ^{1}H via the ^{1}H–^{1}H dipolar coupling. The spin temperature model is thus most appropriate when the relaxation is fast relative to the level-crossing time at frequencies comparable to the dipolar coupling. If the relaxation is slow, an avoided level-crossing model seems more appropriate.

4.2. T_1 effects

A second effect of the ^{1}H nuclei that can be used to increase the ^{14}N NQR signal is a shortening of the effective ^{14}N T_1. Our two materials allow two different regimes to be studied: ^{1}H $T_1 < {}^{14}$N T_1, and ^{1}H $T_1 \sim {}^{14}$N T_1. The first case applies to the site 2 ^{14}N of diglycine hydrochloride. Site 2 ^{14}N of diglycine hydrochloride has a T_1 of roughly 100 ms for ν_+ and ν_- [25] (ν_+ T_1 $\approx$115 ms, ν_- T_1 $\approx$105 ms at room temperature, 22–23 °C). The site 1 ^{14}N and the ^{1}H both have T_1's roughly 10 ms. The ^{1}H T_1 of 7.8 ± 1.5 ms at 607 kHz and 9.6 ± 1.5 ms at 1116 kHz was measured indirectly at 23–26 °C. The sequence used is shown in Fig. 6A.

Since the ^{1}H T_1 is much shorter than the site 2 ^{14}N T_1, matching the frequencies at a level crossing shortens the effective T_1 between those two ^{14}N energy levels, as long as the ^{1}H–^{14}N dipole coupling is strong enough to provide a sufficiently rapid exchange of energy. Effectively, the ^{14}N can equilibrate to the lattice temperature by a two step connection [11]. For the first step, the ^{1}H relax with a fast T_1 to the lattice temperature. For the second step, the ^{14}N equilibrate with the ^{1}H nuclei via the ^{1}H–^{14}N dipole coupling. The recovery of the ν_+ signal after saturation when the ^{1}H frequency is matched to various ^{14}N frequencies can be seen in Fig. 7A. The shortest effective T_1 is when the ^{1}H frequency is matched to the measured ^{14}N frequency, but there are significant effects for matching to the other two ^{14}N frequencies. The shortening of the ^{14}N T_1 is also seen in Fig. 8, where the entire cycle time of the sequence shown as Fig. 2B has been reduced to 60 ms ($<{}^{14}$N T_1). Clear peaks are seen at the level crossings where the effective ^{14}N T_1 has been reduced (thus increasing the signal seen with the 60 ms cy-

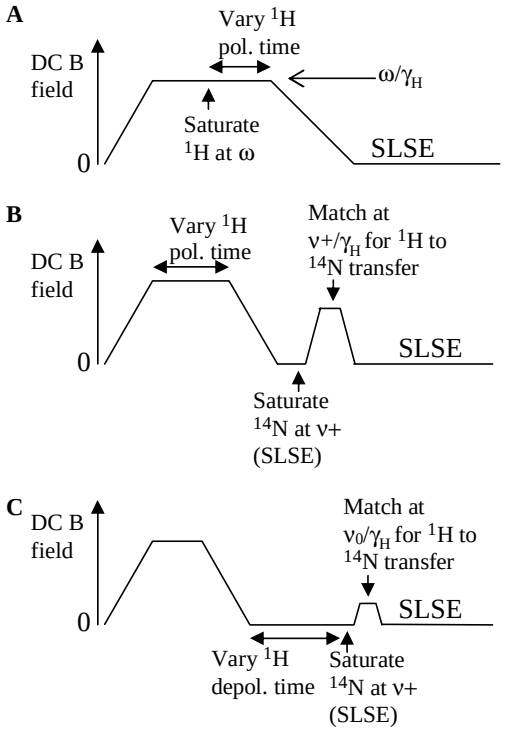

Fig. 6. Sequences used for indirect ^{1}H T_1 measurements: (A) sequence used for diglycine hydrochloride. With magnetic field on, saturate ^{1}H, then vary time for repolarization before the ^{1}H–^{14}N level crossings. ^{1}H polarization seen indirectly as variation in the increase of ^{14}N ν_+ signal from thermal equilibrium (or decrease of ν_- signal). ^{14}N is allowed to fully relax between measurements. (B) Sequence used for TNT. Polarize ^{1}H for a variable length of time, then the field is swept directly to 0 for ^{14}N ν_+ saturation (in a time $\ll$ ^{1}H T_1 at zero field). The field is increased to the ν_+ level crossing to transfer polarization from the ^{1}H to ^{14}N. The field is swept back to 0 to measure transferred polarization at ν_+. (C) Sequence used to indirectly measure ^{1}H T_1 at zero field for TNT. ^{1}H is polarized with magnetic field, then the field is swept down to zero. Next, a variable amount of time is spent relaxing at zero field. Then the ^{14}N ν_+ is quickly saturated, before going to the ν_0 level crossing to transfer polarization from the ^{1}H to ^{14}N. Finally, the field is swept back to 0 to measure transferred polarization at ν_+.

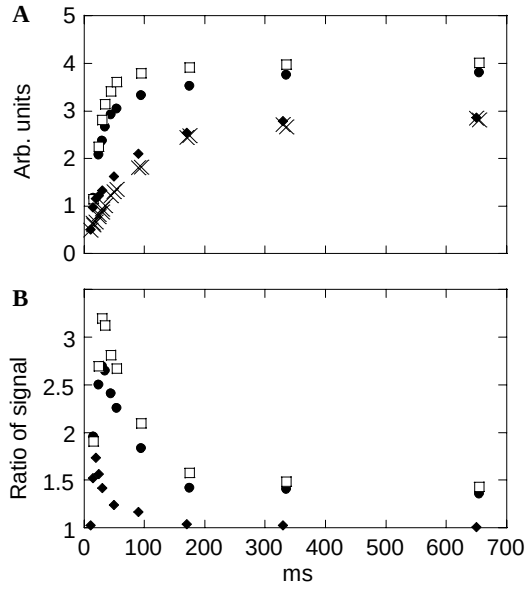

Fig. 7. (A) ν_+ signal recovery after SLSE saturation for diglycine hydrochloride: ×, without any field sweep; ♦, ●, and □, with field sweep to ν_0, ν_-, and ν_+ level crossings, respectively. (B) Ratio of signal with field sweep to signal without any field sweep, for data from part A. Data were taken at 25–27 °C.

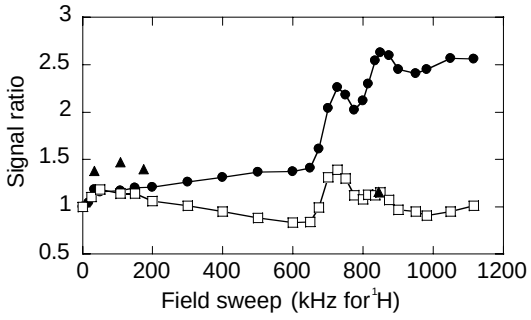

Fig. 8. ^{14}N NQR signal after magnetic field applied for 35 ms ($<$^{14}N T_1) (normalized by signal without any field sweep) as a function of the magnetic field strength (in units of the ^{1}H frequency). Data shown for diglycine hydrochloride site 2 ^{14}N, ν_+ (●) (834 kHz), and ν_- (□) (725 kHz) (Sequence Fig. 2B). Triangles (▲) show the effect on the ν_- NQR signal of field sweeps which alternately sweep on one cycle to the ν_+ level crossing (▲ at 844 kHz on the x-axis), and then sweep on the next cycle to near the ν_0 level crossing (▲'s near 109 kHz on the x-axis). The total cycle time was 60 ms, and the data were taken at 29–33 °C. Error bars are roughly the symbol size, and lines are drawn to guide the eye.

cle time), which were not seen in Fig. 4 when the cycle time was 525 ms (>4 T_1 for ^{14}N). This shortening of the effective ^{14}N T_1 helps increase the signal-to-noise for a fixed amount of time. The best sequence that we found for diglycine hydrochloride was to sweep the magnetic field as follows. First, a 16 ms sweep to 727 kHz (ν_-) where the ^{1}H help to relax the ν_- transition. Second, a 10 ms sweep to the maximum field (1116 kHz) to polarize the ^{1}H. Third, a 10 ms sweep to 844 kHz (ν_+) where the ^{1}H transfer polarization and help to relax the ν_+ transition. Finally, a 15 ms sweep to 0 field. Then the ν_+ signal was measured. These times include both the time spent to change the field (5–15 ms, depending on the amount of field change), and the time spent sitting at the magnetic field. The total cycle time including the SLSE measurement was 70.1 ms. Part of the benefit to the signal-to-noise ratio is from the short cycle time which allows an increased number of cycles to average. For the NQR measurement without a field sweep, the cycle time with the best signal-to-noise was 135.1 ms, while 96.1 and 193.1 ms cycle times had signal-to-noise a few percent worse. This reflects the optimal cycle time for the unperturbed ^{14}N T_1 of ≈115 ms. The benefit of the decreased cycle time used with the field sweep is included in the signal-to-noise ratio for a fixed amount of time by dividing the signal per cycle by the square root of the cycle time. Including both the increased signal per cycle

and the reduced cycle time, the field sweep sequence provided a signal-to-noise ratio for a fixed amount of time 2.5 times better than without a magnetic field sweep. While this sequence was the best measured for the ^{14}N site 2 of diglycine hydrochloride, other variations that included brief stops at the level crossings had increased signals that differed by only a few percent.

For TNT, the ^{1}H T_1 varies significantly with frequency [2]. The long ^{14}N and ^{1}H T_1 relaxation times result in long experiment times for measuring the TNT ^{1}H T_1 by the same methods as we used for diglycine hydrochloride. But because of the small amount of ^{1}H–^{14}N interaction for TNT during a fast field sweep, we could use different sequences to measure the ^{1}H T_1 indirectly in TNT (see Figs. 6B and C). The ^{1}H T_1 is roughly 0.45 s at zero field, 10 s at 550 kHz, and 11 s at 1116 kHz at 14–17 °C. These measurements of ^{1}H T_1 are consistent with [2], which quoted T_1 values at 25 °C: $\sim$ 0.5 s at zero field, increasing to 4.6 s at 200 kHz, and about 30 s at 0.8 T = 34 MHz. The ^{14}N T_1 ranges from 8 to 14 s for the four lines around 843 kHz at zero field and 14 °C, and is $\approx$9 s for the same four lines averaged together at 13 mT = 554 kHz and 16 °C [25]. Since the ^{1}H T_1 is not shorter than the ^{14}N T_1 at the upper level crossings, matching the ν_+ level crossing with initially unpolarized ^{1}H did not shorten the effective ^{14}N T_1 significantly. However, because the ^{1}H T_1 at zero field is 0.45 s, the ^{14}N NQR measurement at zero field can be done in less than the ^{1}H T_1 so that the ^{1}H polarization from high field does not fully relax at zero field. The remaining ^{1}H polarization can be used on the next field sweep cycle. At the beginning of the next field sweep cycle, the magnetic field is turned on, and the ^{1}H frequency is matched to one of the ^{14}N NQR frequencies. The unrelaxed ^{1}H polarization can then be transferred to the ^{14}N nuclei, which have been saturated by the NQR measurement. This helps shorten the effective T_1 recovery of the ^{14}N. When the ^{1}H frequency was matched to the ^{14}N ν_+ region around 843 kHz, with the ^{14}N NQR measurements at zero field taking only 90 ms, the effective ^{14}N T_1 was only 4 s. This shortening of the effective ^{14}N T_1 plus stopping at the ν_- and ν_0 level crossings provided a signal-to-noise ratio increase for a fixed amount of time of a factor of 2.2. Fig. 9 also shows a factor of 2.2 increase of the signal-to-noise ratio when both cycle times are fixed at 5 s, rather than varied to optimize the signal-to-noise. This increase by a factor of 2.2 for the TNT signal-to-noise ratio is not that much larger than the factor of 2.1 mentioned previously from using the maximum field available (26 mT) with the level crossings, but here we have used only 20 mT field.

4.3. Effects of other ^{14}N energy levels

A third effect that can be exploited with small magnetic fields is to use the polarization that remains in

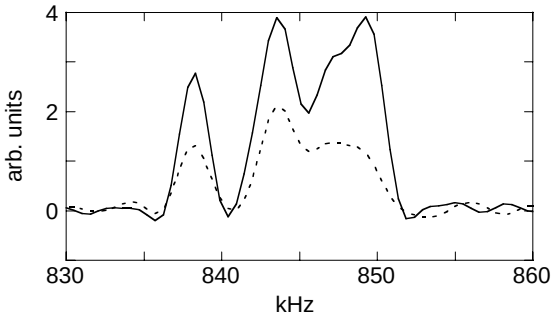

Fig. 9. TNT ^{14}N NQR low-resolution spectra, with (solid line) and without (dotted line) field sweep, measured at 843 kHz with both cycle times set at 5 s. The two spectra are taken with the same number of scans to illustrate the signal enhancement. The total signal integrated over the spectra with the field sweep has increased by a factor of 2.2. For the field sweep, the field is set to the ν_+ level crossing (854 kHz to account for field shift of frequencies) for 4.4 s, then the field is swept down with 100 ms stops at the ν_- level crossings (754, 743, and 715 kHz) and the ν_0 level crossings (132, 107, and 93 kHz). The ^{14}N NQR measurement is done at zero field in 55 ms ($<^{1}$H T_1 at zero field). Spectra taken at 15 °C.

^{14}N energy levels that have not been measured. The ^{1}H nuclei can be used to transfer some of this polarization to the measured transition. For example, measurement of one of the ^{14}N transitions tends to saturate that transition, which equalizes the population in the two energy levels involved in the transition. However, the population of the third ^{14}N energy level has not changed as long as the ^{14}N T_1 relaxation has not been significant. One sequence to demonstrate this is to field sweep to match ν_+ and then measure ν_- at zero field, and then quickly ($<^{14}$N T_1) field sweep to match ν_0 and again measure ν_- at zero field (see ▲'s Fig. 8). The ν_+ field sweep provides a small increase of the ν_- signal, while also polarizing the ν_+ transition, and thus reducing the population in the $|Y\rangle$ state. The population of the $|Y\rangle$ state mostly remains the same during the ν_- measurement because the ν_- transition does not involve the $|Y\rangle$ state and the cycle time is kept less than the ^{14}N T_1. During the subsequent ν_0 field sweep, the thermal equilibration of the ^{1}H transition and the ^{14}N ν_0 transition transfers some of the population from the $|X\rangle$ state to the $|Y\rangle$ state, thus enhancing the ν_- signal (see ▲'s around 100 kHz in Fig. 8). This effect of using polarization remaining in the third ^{14}N energy level was also seen in TNT. Starting with unpolarized ^{1}H, a field sweep from 0 field to the ν_0 level crossings (107 and 96 kHz, 100 ms each) benefits the ν_- signal at 743 kHz by 40% for a 5 s cycle time. This can be explained as follows. At the ν_0 level crossings, the unpolarized ^{1}H nuclei help to equalize the population of the two states involved in the ν_0 transition, $|Y\rangle$ and $|X\rangle$. The ν_- signal ($|X\rangle \rightarrow |Z\rangle$) thus benefits from the polarization of the $|Y\rangle$ state. This technique of using the third ^{14}N energy level can benefit the ^{14}N NQR signal, while requiring only a tiny

magnetic field (2.5 mT). We should also mention that another possible way to use the polarization of the third ^{14}N energy level is to apply an inversion pulse or saturation of the ν_0 transition, instead of the field sweep to the ν_0 level crossings.

In TNT, there are 6 nitrogen sites with different NQR frequencies for each crystalline type (monoclinic and orthorhombic) (see Table 1). The polarization of any one ^{14}N frequency could potentially be replenished by transfer from other nearby ^{14}N crystal sites. It is possible for level crossing to happen directly between different ^{14}N sites, depending on the geometry of the electric field gradient tensors. However, since the ^{14}N–^{14}N dipole couplings are small (estimated as ~10 Hz in TNT), a direct ^{14}N–^{14}N process will be slow at best. Instead, the ^{1}H can be used to move polarization from one ^{14}N site to another. We found that a sequence designed to use this process by stopping at the level crossings for other ^{14}N sites could provide an increase of the signal-to-noise ratio by a factor of 2.1. This sequence started with two magnetic field stops in the vicinity of other ^{14}N sites (100 ms each at 873 and 880 kHz). Then, there was a 2.3 s stop in the ν_+ region of the measured sites (854 kHz). Finally, the field was swept down with 100 ms stops at ν_- (770 and 715 kHz) and ν_0 level crossings (132, 107, and 93 kHz). The ^{14}N signal in the 835–855 kHz region was measured at zero field at 843 kHz. However, because of the closely spaced lines of TNT, it is not clear whether the benefit of the additional stops arises from the level crossings of other ^{14}N sites or just because the stops are also near the level crossings of the measured sites. Measurement of the signal enhancement as a function of the position of a magnetic field stop around ν_+ did not resolve the ν_+ level crossings of different ^{14}N sites. The best overall sequence that we found for TNT ν_+ signal was as described in the caption of Fig. 9: to match the field to the ν_+ level crossing and then stop at the ν_- and ν_0 level crossings as the field is swept to zero.

5. Conclusions

Small amounts of magnetic field can be produced by a simple solenoid to create and manipulate ^{1}H polarization in several ways to increase the signal-to-noise ratio of low frequency ^{14}N NQR. The increase that can be attained depends on a number of factors, including the magnetic field available, the ratio of the T_1's of ^{1}H and ^{14}N, and the number of ^{1}H nuclei per ^{14}N nucleus. We have found that the benefit to the signal-to-noise ratio can be significant even for very small magnetic fields, providing much more benefit than a first glance approach of comparing the achievable ^{1}H frequency to the measured ^{14}N frequency. In these experiments, we demonstrated an increase of 2.5 in the signal-to-noise ratio for a fixed amount of time for the ^{14}N site 2 (the slower relaxing site) of diglycine hydrochloride using 26 mT and an increase of 2.2 for the multiple ^{14}N sites of TNT near 843 kHz using 20 mT.

Acknowledgments

This research was performed while the author held a National Research Council Research Associateship Award at the U.S. Naval Research Laboratory. Funding was provided by the Office of Naval Research (ONR) and the U.S. Army Night Vision Lab. One of us (KLS) would like to acknowledge a NSF ADVANCE award.

References

[1] A.N. Garroway et al., Remote sensing by nuclear quadrupole resonance, IEEE T. Geosci. Remote 39 (2001) 1108.
[2] R. Blinc, J. Seliger, D. Arčon, P. Cevc, V. Žagar, H–^{14}N double resonance of TNT from a land mine, Phys. Stat. Sol. A 180 (2000) 541.
[3] M. Nolte, A. Privalov, J. Altmann, V. Anferov, F. Fujara, ^{1}H–^{14}N cross-relaxation in trinitrotoluene-a step toward improved landmine detection, J. Phys. D: Appl. Phys. 35 (2002) 939.
[4] V.S. Grechishkin, R.V. Grechishkina, A.A. Shpilevoĭ, A.A. Persichkin, Hoon Heo, Remote detection of double nuclear quadrupole resonance spectra, Opt. Spectrosc.-USSR 94 (2003) 352.
[5] R. Blinc, T. Apih, J. Seliger, Nuclear quadrupole double resonance techniques for the detection of explosives and drugs, Appl. Magn. Reson. 25 (2004) 523.
[6] V.S. Grechishkin, V.P. Anferov, N.Ja. Sinjavsky, Adiabatic demagnetization and two-frequency methods in ^{14}N quadrupole resonance spectroscopy, in: J.A.S. Smith (Ed.), Advances in Nuclear Quadrupole Resonance, vol. 5, John Wiley, London, 1983, pp. 13–23.
[7] J. Luznik, J. Pirnat, Z. Trontelj, Polarization enhanced ^{14}N NQR detection with a nonhomogeneous magnetic field, Solid State Commun. 121 (2002) 653.
[8] T. Hahn, M.J. Buerger, The crystal structure of diglycine hydrochloride, $2(C_2H_5O_2N)\cdot HCl$, Z. Kristallogr. 108 (1957) 419; S. Natarajan, C. Muthukrishnan, S. Asath Bahadur, R.K. Rajaram, S.S. Rajan, Reinvestigation of the crystal structure of diglycine hydrochloride, Z. Kristallogr. 198 (1992) 265; J.W. Faamau, E.R.T. Tiekink, New data for diglycinehydrochloride, Z. Kristallogr. 204 (1993) 277.
[9] A. Abragam, Principles of Nuclear Magnetism, Clarendon Press, Oxford, 1961, p. 166.
[10] D.T. Edmonds, Nuclear quadrupole double resonance, Phys. Rep. 29 (1977) 233.
[11] D.H. Smith, R.M. Cotts, Nitrogen electric quadrupole and proton magnetic resonances in thiourea, J. Chem. Phys. 41 (1964) 2403.
[12] G.W. Leppelmeier, E.L. Hahn, Nuclear dipole field quenching of integer spins, Phys. Rev. 141 (1966) 724.
[13] A. Naito, A. Root, C.A. McDowell, Combined sample rotation and multiple-pulse NMR spectroscopic studies on protons bonded to ^{14}N nuclei in solid amino acids, J. Phys. Chem. 95 (1991) 3578.
[14] R.A. Marino, S.M. Klainer, Multiple spin echos in pure quadrupole resonance, J. Chem. Phys. 67 (1977) 3388.

[15] R.A. Marino, R.F. Connors, L. Leonard, Nitrogen-14 NQR study of energetic materials, U.S. Army report: U.S. NTIS AD-A119844.
[16] R.A. Marino, R.F. Connors, Orthorhombic and monoclinic TNT: a nitrogen-14 NQR study, J. Mol. Struct. 111 (1983) 323.
[17] G. Grössl, F. Winter, R. Kimmich, Optimisation of magnet coils for NMR field-cycling experiments, J. Phys. E: Sci. Instrum. 18 (1985) 358.
[18] D. Stephenson, J.A.S. Smith, ^{14}N quadrupole double resonance in 2-, 3- and 4-nitrobenzoic acids, J. Chem. Soc., Faraday Trans. 2 83 (1987) 2123.
[19] V.P. Anferov, S.V. Anferova, V.S. Grechishkin, N.J. Sinjavsky, Method of adiabatic demagnetization in NQR, J. Mol. Struct. 83 (1982) 89.
[20] V.P. Anferov, V.S. Grechishkin, S.V. Grechishkina, NQR-NMR double resonance, Izv. An. SSSR Fiz. 42 (1978) 2164;
V.S. Grechishkin, N.Y. Sinyavskii, Line intensities in NQR-NMR double resonance, Izv. An. SSSR Fiz. 42 (1978) 2176.
[21] D. Stephenson, J.A.S. Smith, Nitrogen-14 quadrupole cross-relaxation spectroscopy, Proc. R. Soc. Lon. Ser.-A 416 (1988) 149.
[22] M. Goldman, Spin Temperature and Nuclear Magnetic Resonance in Solids, Clarendon Press, Oxford, 1970, p. 171.
[23] J.W. Zwanziger, S.P. Rucker, G.C. Chingas, Measuring the geometric component of the transition probability in a two-level system, Phys. Rev. A 43 (1991) 3232.
[24] A.J. Vega, MAS NMR spin locking of half-integer quadrupolar nuclei, J. Magn. Reson. 96 (1992) 50.
[25] Diglycine hydrochloride and TNT ^{14}N NQR T_1's were measured by the magnetization recovery after a spin-lock spin-echo (SLSE) sequence was used for saturation. Within error, the biexponential behavior possible in spin 1 NQR [26] was not seen for either diglycine hydrochloride site 2 or TNT ^{14}N NQR T_1 relaxation curves.
[26] G. Petersen, P.J. Bray, ^{14}N nuclear quadrupole resonance in sodium nitrite, J. Chem. Phys. 64 (1976) 522.